Original Manuscript

Journal of Vibration and Control
2023, Vol. 0(0) 1–13

DOI: 10.1177/10775463231206601
journals.sagepub.com/home/jvc


Model-free robust decentralised control of multi-input-multi-output nonlinear interconnected dynamic systems

Quanmin Zhu[1], Ruobing Li[1], Jianhua Zhang[2], and Baiyang Shi[1]

Abstract

This study presents a generalised framework for model-free robust decentralised control (MFRDC) of interconnected MIMO dynamic systems, with the goal of significantly reducing complexity in model-based design. A model-free robust sliding mode control, by Lyapunov differential inequality, is presented to achieve simultaneous nonlinear, dynamic, interaction/coupling inversion/cancellation (NDII) for such MIMO systems, which treats the plant/process as a total uncertainty from input to output. The U-control platform is presented, to integrate separately independently designed NDII and an invariant controller (IC) into a complete double loop control system. The associated robust stability and other properties are analysed to provide reference for applications. Two simulated tracking control tests are presented for functionally numerical demonstration, validation of the analytical results and illustration of the transparent procedure for general expansion/applications. These are: a coupled inverted pendulum and a two-input and two-output (TITO) non-affine nonlinear dynamic plant.

Keywords

model-free robust decentralised control, model-free sliding mode control, nonlinear, dynamics, interaction/coupling inversion/cancellation, U-control platform, control of coupled inverted pendulums

1. Introduction

With technology advances and ever-evolving cooperation, interconnected manmade systems (e.g. engineering operations in motion and process) show a tendency towards increasing operational procedures and products in scale and complexity. Such systems exist widely and are proliferating: for example, distributed energy resources in power grids (Mukherjee et al., 2020), robot joint subsystems with interconnected dynamic couplings (Dong et al., 2019), coupled inverted pendulums (Ding et al,. 2021), and networked control systems (Bakule, 2014). Such subsystem interconnection also characterises many natural systems and non-engineering organisational operations, such as collective motion in biology, swarm intelligence, cooperative estimation, economic equilibria, and social networks/interactions (Antonelli, 2013). Distributed/decentralised control of such interconnected dynamic systems has been an active research and application topic (Antonelli, 2013). Compared with centralised control, decentralised/distributed control has been shown to display the following characteristics, (1) generally simpler and cheaper in design and cost, (2) generally stronger in fault tolerance, and (3) generally facilitating large network control strategies and algorithms. Conversely, the decentralised control requires more comprehensive specialist knowledge in design and analysis (Bakule, 2008). It has been observed from research publications that associated interdisciplinary research fields are increasingly attracting researchers and practitioners from different subject communities (Antonelli, 2013; Zhang et al. 2020). This study focuses on critical review of some representatively related approaches to justify motivation: model-free robust decentralised control and some major contributions.

[1]School of Engineering, University of the West of England, Bristol, England
[2]School of Information and Control Engineering, Qingdao University of Technology, Qingdao China

Received: 14 March 2023; revised: 28 August 2023; accepted: 23 September 2023

Corresponding author:
Quanmin Zhu, School of Engineering, University of the West of England, Frenchay Campus, Bristol BS16 1QY, England.
Email: quan.zhu@uwe.ac.uk

1.1. Decentralised control of interconnected systems

The most popular class of the approaches is to take the system plant nominal models as reference to design the control systems with specified control objectives in transient and steady state responses, which inaccuracy and/or variation of the parameters of the models are treated as uncertainties. For the model-based control, including dealing with nominal models and time varying models (Chen et al., 2021), and the challenging issues in the control are related with nonlinear dynamics, dynamic coupling effects, and a commonly agreed critical challenge in determining appropriate configurations/solution procedures so that each subsystem achieves the specified performance in the presence of uncertainty, such as parameter variation, unmodeled components, and unknown interconnections. Some selected approaches dealing with interconnection-induced difficulties are quoted here: neural network topologies have been presented for connection of structures storage and the dissipativity of subsystems (Jokić and Nakić, 2019). Model-based sliding mode techniques (Ding et al., 2021) have been successfully applied to decentralised control of uncertain nonlinear interconnected systems. Neural network enhanced control has been another popular approach in improving the robustness/adaptive functionalities (Li et al., 2021). Graph theory has been an important tool for decentralised adaptive fault-tolerant control of a class of strong interconnected nonlinear systems (Ma and Xu 2020). Fault detection/accommodation in interconnected systems has also attracted attention (Ma and Xu 2020; Zhao and Polycarpou 2021). A new and worthwhile result for dealing with output constraints is being pursued in academic research and applications (Hua et al., 2021). In summary, model-based approaches have achieved various significant results and will continue to be the predominant methodology in research and applications. However, as every model-based approach has a common drawback, that is, sensitivity to model uncertainty, additional effort, and computational cost is required in the control system's design. To the authors' best knowledge, addressing of the problems in alternative approaches, model-free control methodology has been studied, but not in-depth, with the interconnected system topologies.

A popular approach in coping with uncertainties has been the use of adaptive control to achieve model-free decentralised control (Dong et al. 2019). However strictly speaking this is not a type of model-free control, as almost all adaptive control publications still use online estimated models for controller design. The bottleneck issue of not having model-free decentralised control of interconnected plants lies in the lack of proper configuration and mathematical formulation dealing with nonlinear dynamic coupling between states/outputs. The other class of the representative approach is to use data-driven based learning control to deal with distributed systems (Mukherjee et al. 2020). Obviously, this approach is time-consuming due to use of reinforcement learning to calculate the optimal control gains. Improvement of computational efficiency could therefore be another motivation for new studies.

It should be emphasised that even though this study has focused on model-free control, the importance of the modelling role in facilitating control system design is not denied, especially in simulation studies. In practice, particularly in industrial applications, great effort has been made on experiments and tests for modelling and understanding of underlying plants/processes prior to control system design. Model-free control system design still requires fundamental system model knowledge, such as stable, controllable, observable, dynamic order, delayed time, actuator saturation, etc. even not requiring accurate/nominal quantitative models. In a broad sense, model-free control is a supplement to model-based control and reduction of tedious modelling work and the control design complexity.

1.2. U-control – robust double dynamic inversion

U-control has been progressed from model-based (matched and mismatched) to model-free design. The kernel foundation of the method is double dynamic inversion to provide simplicity and generality (solutions) from complexity (problems). Some selected publications are presented here for reference: Model-based U-control (Zhu and Guo 2002) achieves general linear pole-placement control by integration of solving Diophantine equation and nonlinear dynamic inversion, one work (Li et al. 2020) derives a general procedure for U-model-based dynamic inversion, one study (Zhang et al. 2020) establishes the U-Model and U-control methodology for nonlinear systems, a new publication propose a robust U-control of nonlinear dynamic models with disturbance observer (Li et al. 2022). For model-free U-control: Zhu (2021) presents a foundation platform to develop model-free sliding mode control (MFSMC) for dynamic inversion, another work (Zhu et al. 2023) applies the MFSMC to a new configuration of composite nonlinear feedback control for nonlinear systems with input saturation. There have been several application-based studies, observed based U-control of COVID-19 (Wei et al., 2022), U-control based under-actuated coupled nonlinear adaptive control model for multivariable unmanned marine robotics (Hussain et al. 2019), and U-model enhanced trajectory tracking control of quadrotors (Li et al. 2023). With U-control insight, researchers have tried to provide supplementary references to various well-established control methods in terms of generality and simplicity. For U-control enhanced decentralised systems, this is the first study with novelty in solution of robust model-free decoupling.

1.3. Justification of the study

Motivated by the above analysis, this study tries to remove control system design dependence on plant models (by dynamic inversion), increases the system robustness and decoupling effectiveness (through model-free SMC), and expand the generality (through model-free) and simplicity in design and implementation (U-control, NDII, and IC). The study also provides computational demonstration on the selected bench tests for understanding and applications. The significant contributions from the study are as follows:

(1) To the author's best knowledge, this is the first study to take a dynamically interconnected nonlinear plant as a total uncertainty, to propose the nonlinear, dynamic, and interconnection inversion (NDII) to establish a foundation for generalised model-free robust decentralised control.
(2) Conceptual configuration of the NDII only requires measured errors and their derivatives vector in a closed loop control of a bounded input and bounded output (BIBO) system. Analytical generalisation of the NDII is derived from an expanded SISO model-free sliding model control (MFSMC), which adds dynamic decoupling to accommodate interconnections/couplings between the subsystem dynamics.
(3) Simulation studies with U-control platforms take computational experiments with interconnected/coupled nonlinear dynamic plants. This is not only used to validate the analytical results, but also to provide transparent guidance for future applications.

The rest of the study includes four sections. Section 2 presents preliminaries for the reference conducting the follow up development. Section 3 derives NDII to lay the foundation for model-free control and analyses the associated properties to provide reference for applications. Section 4 presents the MFRDC framework and proves the associated properties based on the U-control platform. Section 5 conducts bench tests of two selected examples on a comprehensive computational experimental platform, to demonstrate the analytical results, validate the control system configuration of the functional block connections, illustrate a transparent application procedure, and compare with the other representative approaches. Section 6 summarises the study with its major outcomes and potential impacts and suggests future research directions. An appendix shows some extra simulation results generated from the other comparative approach, which otherwise will be over the paper length limits.

2. Preliminaries

2.1. Interconnected systems

Consider a general model for describing interconnected nonlinear MIMO systems (Ding et al., 2021)

$$\Sigma_1:\begin{cases}\dot{x}_i=f_i(x_i)+g_i(x_i)(u_i+\alpha_i(x_i))+\beta_i(x)\\ y_i=h_i(x_i)\quad i\in\mathbb{Z}[1,\cdots,N]\end{cases}\tag{2.a}$$

where for the ith subsystem, the triplet $\{x_i\in\mathbb{R}^{n_i},\ u_i\in\mathbb{R},\ y_i\in\mathbb{R}\}$ denotes the state, control input, and output, respectively, $f_i:\mathbb{R}^{n_i}\to\mathbb{R}, g_i\neq 0:\mathbb{R}^{n_i}\to\mathbb{R}$ denote the nominal dynamics, $\alpha_i:\mathbb{R}^{n_i}\to\mathbb{R}, \beta_i:\mathbb{R}^{\sum_{i=1}^{N}n_i}\to\mathbb{R}$ denote the matched uncertainties and the known/unknown interconnections, respectively. Take $x=col\{x_1\cdots x_n\}\in\mathbb{R}^{\sum_{i=1}^{N}n_i}$ and assume the Lipschitz continuity satisfied with the system model. This study will treat the whole model as uncertainty to develop a new model-free control framework.

2.2. Model-free U-control systems

Figure 1 shows the model-free U-control system, which is functionally expressed as (Zhu, 2021)

$$\begin{aligned}\Sigma_U:\left(F,C\left(C_{IV},\widehat{P}^{-1}\right),P\right)&\Leftrightarrow\left(F,C_{IV},I_n\in C_{NDI}\left(\widehat{P}^{-1},P\right)\right)\\&\Leftrightarrow(F,C_{IV},I_n)\end{aligned}\tag{2.b}$$

where F denotes the configuration of the U-control system. For a general model-unknown plant $P\in\mathbb{R}^n$, the objective of the U-control system is to use double loop of control configuration, with independent, separate design, taking the inner loop for nonlinear dynamic inversion/cancellation $C_{NDI}(\widehat{P}^{-1},P)$ via a model-free sliding mode control $\widehat{P}^{-1}=$ MFSMC to achieve the nth order identity matrix $C_{NDI}(\widehat{P}^{-1},P)\in I_n$, and taking the outer loop for linear dynamic inversion to realise a specified whole control system performance via a linear invariant controller C_{IV}. Thus, the invariant controller generates the desired state vector for the inner state feedback control loop. For state feedback control, if full states are not available, a state observer, for example extended state observe (*ESO*), can be used for state estimation from the controller input and the measured system output (Guo and Zhao, 2011).

This study uses the U-control platform to integrate the functional components (C_{IV},C_{NDI},P) into a proper control framework, and to conduct simulation

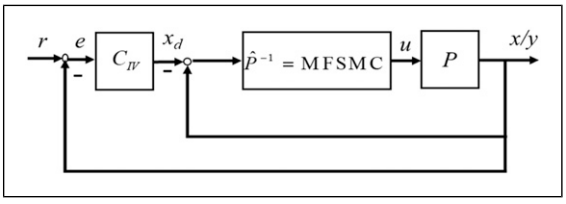

Figure 1. Model-free U-control platform.

validation/demonstration of the designed control systems.

3. Model-free nonlinear dynamics, and interconnections inversion

Proposition 3.1. SISO model-free nonlinear dynamic inversion can be expandable to interconnected MIMO systems, in which coupled dynamics are treated as uncertainties. Accordingly, for MIMO systems, this type of inverter covers the inversion/cancelation of nonlinearities, dynamics, plus interconnections/couplings.

3.1. Design of system output-based sliding function

Consider a further generalised system description of an input-output model from the interconnection state space model of (2.1)

$$\Sigma_4 : y_i^{(n_i)} = H_i(y, u_i) \quad i \in \mathbb{Z}[1, \cdots, n] \tag{3.a}$$

where $y = col\{y_1 \cdots y_n\} \in \mathbb{R}^{\sum_{i=1}^{N} n_i}$, $H_i : \mathbb{R}^{\sum_{i=1}^{N} n_i} \to \mathbb{R}$ is a continuously differentiable function, a mapping from the input space to the output space. Assume the inverse mapping $u_i = H_i^{-1}(y_i^{(n_i)})$ exist. For taking model-free NDII, assume (1) the dynamic order of each subsystem $n_i \in \mathbb{Z}^+$ is known, (2) the corresponding output derivatives, up to $y^{(n_i-1)} \in R$, of the subsystem are available, (3) $H_i \in A : u_i \to y_i$, where A is the algebra of all polynomials on the irreducible real affine variety y, an unknown mapping and treated as a whole uncertainty in the study, and (4) the plant set is bounded input bounded output (BIBO), $|u| \le B_u, |y| \le B_y, \forall t \in \mathbb{R}$, B_u, B_y are the corresponding bounds.

To design the model-free SMC, take a single line of the subsystem in (3.a), assign the desired output $y_{id}(t) : \mathbf{D} \to \mathbb{R}$ being continuously differentiable up to $y^{(n_i-1)} \in R$, then the corresponding tracking error is defined as

$$e_i(t) = y_i(t) - y_{id}(t) \quad i \in \mathbb{Z}[1, \mathbb{L}, n] \tag{3.b}$$

And then define the n_ith order error vector with

$$\begin{aligned} \tilde{y}_i &= \left[e_i \ (e_i)^{(1)} \ \cdots \ (e_i)^{(n_i-1)}\right]^T \\ &= \left[y_i - y_{id} \ (y_i - y_{id})^{(1)} \ \cdots \ (y_i - y_{id})^{(n_i-1)}\right]^T \in \mathbb{R}^{n_i} \ i \in \mathbb{Z}[1, \mathbb{L}, n] \end{aligned} \tag{3.c}$$

Accordingly, setup a general sliding mode function in expression of

$$\sigma_i(\tilde{y}_i) = C_i \tilde{y} + \xi_i : \mathbb{R}^{n_i} \to \mathbb{R} \quad i \in \mathbb{Z}[1, \mathbb{L}, n] \tag{3.d}$$

where $C_i \in \mathbb{R}^{1 * n_i}$ is assigned to make the sliding mode function a Hurwitz stable polynomial and ξ_i is a term to reflect the interactions with the other outputs $y_j, \forall j \ne i$ and $|\xi_i| < |\xi|$. Alternatively, the sliding mode function can be expressed as $\sigma_i(\tilde{y}_i) - \xi_i = C_i \tilde{y} : \mathbb{R}^{n_i} \to \mathbb{R} \quad i \in \mathbb{Z}[1, \cdots, n]$.

Remark 3.1. The decentralised sliding mode functions construct a basis for proposing a mechanism to decouple the dynamic interactions in the decentralised control.

3.2. Nonlinear, dynamic, interaction/coupling inversion/cancellation

Theorem 3.1. For the general interconnected dynamic plant (3.a) (let $\Sigma_4 = P$ for the consistence with that shown in Figure 1), there exists a diagonal matrix controller $\exists \widehat{P}^{-1} \in \text{diag}\{\widehat{p}_1^{-1} \cdots \widehat{p}_n^{-1}\}$, and the controller output is $U : \ \exists(\widehat{P}^{-1}) \in \text{diag}\{u_1 \quad \cdots \quad u_n\}$. So that a feedback control system $C_{NDII}(\widehat{P}^{-1}, P)$, can achieve $C_{NDII}(\widehat{P}^{-1}, P) \to^{asymp} I_n$, which implies nonlinear, dynamic, and interconnection inversion/cancellation (NDII).

Proof. Define $\widehat{P}^{-1} : \text{diag}\{mfsmc_1 \quad \cdots \quad mfsmc_n\}$, the corresponding MFSMC controller outputs can be assigned in the general form of

$$u_i = \begin{cases} u_{isw} = -k_{ig} \text{sgn}(\sigma_i) (\dot{\sigma}_i \sigma_i < 0) & \forall |\sigma_i| > \delta_i \\ u_{ieq} = g_i(\dot{\sigma}_i = \rho_i(\sigma_i, u_i) \cap \dot{\sigma}_i \sigma_i < 0) & \forall |\sigma_i| \le \delta_i \end{cases}, i = [1, \cdots n] \tag{3.e}$$

where $g_i : \rho_i(*) \to u_i$, $\dot{\sigma}_i - \rho_i(\sigma_i, u_i) = 0$ is the equation for the model-free solutions while satisfies the Lyapunov differential inequality $\dot{\sigma}_i \sigma_i < 0$. It should be noted that for conventional model-based equivalence, control $\dot{\sigma}_i = 0 \to \rho_i(\sigma_i, u_i) = 0$, and $\rho_i(\sigma_i, u_i)$ is the nominal model. To prove Lyapunov stability conditions $V = \sigma^2 > 0$, $\dot{V} = \dot{\sigma}\sigma < 0$, assign the Lyapunov function for each line of the subsystems as V_i and the derivative $\dot{V}_i$ below

$$\begin{aligned} V_i &= \frac{1}{2}\sigma_i^2 > 0 \\ \dot{V}_i &= \dot{\sigma}_i \sigma_i < 0 \end{aligned} \quad i = [1, \cdots n] \tag{3.f}$$

Consequently, the whole system Lyapunov candidate function is defined as

$$V = V_1 + V_2 + \cdots V_n = \frac{1}{2} \sum_{i=1}^{n} \sigma_i^2 \tag{3.g}$$

And the derivative is,

$$\dot{V} = \dot{\sigma}_1 \sigma_1 + \dot{\sigma}_2 \sigma_2 + \cdots \dot{\sigma}_n \sigma_n = \sum_{i=1}^{n} \sigma_i \dot{\sigma}_i \tag{3.h}$$

First, prove the Lyapunov stability conditions for a single line of the subsystems. Rewrite (3.e),

$$u_i = \begin{cases} u_{isw} = -k_{ig}\mathrm{sgn}(\sigma_i)(\dot{\sigma}_i\sigma_i<0) & \forall|\sigma_i|>\delta_i \\ u_{ieq} = g_i(\dot{\sigma}_i=\rho_i(\sigma_i,u_i)\cap\dot{\sigma}_i\sigma_i<0) & \forall|\sigma_i|\le\delta_i \end{cases}, i=[1,\cdots n] \tag{3.i}$$

where for the equivalent control u_{ieq}, the first condition is for model-free assignment of the equivalent control and the second condition is for satisfying Lyapunov stability criterion. That is, expressed as

$$u_{ieq} \in \begin{cases} \dot{\sigma}_i = \rho_i(\sigma_i, u_i) \\ \dot{\sigma}_i\sigma_i < 0 \end{cases}, \forall|\sigma_i| \le \delta_i, \quad i = [1,\cdots n]$$

For the switching control u_{isw}, the proof follows the conventional proof of the SMC (Slotine and Li, 1991).

Therefore, the whole system under model-free NDII is Lyapunov stable, satisfying,

$$\begin{aligned} V &= \frac{1}{2}\sum_{i=1}^{n}\sigma_i^2 > 0 \\ \dot{V} &= \sum_{i=1}^{n}\sigma_i\dot{\sigma}_i < 0 \end{aligned} \tag{3.j}$$

This indicates, while on the sliding mode, $\lim_{t\to\infty} e_i(t) = \lim_{t\to\infty}(y_i(t) - y_{di}(t)) = 0, \quad i \in \mathbb{Z}[1,\cdots,n]$, which output $y_i(t)$ of plant (3.a) remaining on the sliding mode follows the desired output $y_{id}(t)$ asymptotically. Therefore,

$$[y_1\cdots y_n]^T = I_n[y_{1d}\cdots y_{nd}]^T \to C_{NDII}\left(\widehat{P}^{-1}, P\right) \xrightarrow{asymp} I_n \tag{3.k}$$

Remark 3.2. There are various choices of determining $u_{ieq} = g_i(\dot{\sigma}_i = \rho_i(\sigma_i, u_i)\cap\dot{\sigma}_i\sigma_i<0)$. For example, the proportional gain selection (Zhu 2021), as an example, shows below,

$$u_i = \begin{cases} u_{isw} = -k_{ig}\mathrm{sgn}(\sigma_i) & \forall|\sigma_i|>\delta_i \\ u_{ieq} = -k_{il}\sigma_i - \varepsilon_i & \forall|\sigma_i|\le\delta_i \end{cases}, i = [1,\cdots n] \tag{3.l}$$

where the constant gains $\begin{matrix}|\sup(H_i)|<k_{ig}<|\sup(k_{ig})|, \forall u_{isw} \\ |\sup(H_i)|<k_{il}<|\sup(k_{il})|, \forall u_{ieq}\end{matrix}$, and $|\sup(H_i)|$ is the ith plant output bound, and $|\sup(k_{ig})|, |\sup(k_{il})|$ are the controller saturation bounds. The sliding mode function σ_i is defined in (3.d), δ_i is the sliding mode boundary layer thickness around the sliding surface. k_i is a time varying gain, and ε_i, $\forall\sigma_i = const, \varepsilon_i = const$, virtual variable is used for matching the equality $\dot{\sigma}_i = \sum_{j=1}^{n_i-1} c_{ij}e_i^{(j)} + y_i^{(n_i)} - y_{id}^{(n_i)} = \sum_{j=1}^{n_i-1} c_{ij}e_i^{(j)} + f_i(*) - y_{id}^{(n_i)} = k_i\sigma_i + \varepsilon_i + u_i$.

Remark 3.3. Regarding the NDII convergent speed, which is determined by the selection of the function $\rho(\sigma,u)$, and accordingly, the control input u_i: $\rho_i(*)\to u_i, \forall\dot{\sigma}_i\sigma_i<0$. Here two examples are picked up to show the convergence speed of C_{NDII} $(\widehat{P}^{-1}, P) \xrightarrow{asymp} I_n$.

1) Proportional control, $u_i = \begin{cases} u_{isw} = -k_{ig}\mathrm{sgn}(\sigma_i) & \forall|\sigma_i|>\delta_i \\ u_{ieq} = -k_{ip}\sigma_i - \varepsilon_i & \forall|\sigma_i|\le\delta_i \end{cases}, i = [1,\cdots n]$, which is derived from $\dot{\sigma}_i = \rho(\sigma_i,u_i) = k_i\sigma_i + \varepsilon_i = -(k_{ip}-k_i)\sigma_i + \varepsilon_i$. Taking up the Laplace transform $\mathrm{L}(*)$ of the differential equation gives $\mathrm{L}(\sigma_i) = \frac{\varepsilon_i}{s+(k_{ip}-k_i)} \quad (k_{ip}-k_i)>0$, which the convergent speed is determined by the 1st order dynamic system time constant $1/(k_{ip}-k_i)$. It asymptotically exponentially converges to $\lim_{t\to\infty}\sigma_i = \lim_{s\to 0}\mathrm{L}(\sigma_i) = \varepsilon_i/(k_{ip}-k_i)$ from the Laplace final value theorem.
2) The Proportional and integral control, $u_i = \begin{cases} u_{isw} = -k_{ig}\mathrm{sgn}(\sigma_i) & \forall|\sigma_i|>\delta_i \\ u_{ieq} = -k_{ip}\sigma_i - k_{ii}\int\sigma_i - \varepsilon_i & \forall|\sigma_i| \end{cases}$ $\le\delta_i i = [1,\cdots,n]$, which is derive from $\dot{\sigma}_i = \rho(\sigma_i,\ u_i) = k_1\sigma_i + k_2\int\sigma_i + u_i + \varepsilon_i = -(k_{ip}-k_1)\sigma_i - (k_{ii}-k_2)\int\sigma_i + \varepsilon_i$. Taking up the Laplace transform $\mathrm{L}(*)$ of the differential equation gives $\mathrm{L}(\sigma_i) = \frac{s\varepsilon_i}{s^2+(k_{ip}-k_1)s+(k_{ii}-k_2)}$, which the convergent speed is determined by the second order system natural frequency $\omega = \sqrt{(k_{ii}-k_2)}$. It asymptotically exponentially converged to $\lim_{t\to\infty}\sigma_i = \lim_{s\to 0}\mathrm{L}(\sigma_i) = 0$ from the Laplace final value theorem.

4. Model-free robust decentralised control

Figure 2 shows the MFRDC system configuration. From the decentralised control system design convention (Bakule 2008), this MFRDC is configured with the following two phases.

Specification phase:

1) Plant priori information, including assumptions of the plant being observable, controllable, stabilisable, and BIBO, and the plant, except the dynamic order, is treated

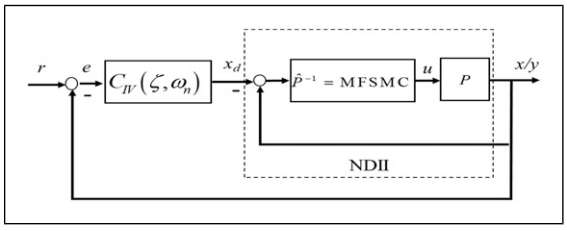

Figure 2. MFRDC system configuration.

as a whole uncertainty in the study. Therefore, this is a type of mode-free control system design.

2) The control goals for the tracking requirement include (1) the NDII with $C_{NDII}(\widehat{P}^{-1}, P) \xrightarrow{asymp} I_n$ in the inner loop, (2) the whole system dynamic performance governed by a linear dynamic matrix $C_{IV}{}^{n*n} = \text{diag}[C_{1IV}\mathbb{L}C_{nIV}]$, for example a second order dynamic sub-controller $C_{iIV}(\zeta_i, \omega_{in})$, in the outer loop, and the system output steady state error $\lim_{t\to\infty} e_i(t) \to 0, \forall e_i(t) = y_i(t) - y_{di}(t)$ and $\lim_{t\to\infty} \sum_{i=1}^{n} |e_i(t)| \to 0$. The decoupling, stabilisation, and robustness are embedded within the designed control system.

Design phase:

1) Design the two dynamic inverters (inner loop/NDII, outer loop tracking performance specification) separately/independently to generate the control input to drive the system with the specified requests.
2) Determine the desired state vector for the NDII from the state space equation realisation from $C_{IV}(\zeta, \omega_n)$.
3) Connect the components with U-control configuration $\Sigma_U : (F, C(C_{IV}, \widehat{P}^{-1}), P) \Leftrightarrow (F, C_{IV}(\zeta, \omega_n), I_n \in C_{NDII}(\widehat{P}^{-1}, P))$.
4) Assume the outputs and their derivatives are available for feedback control. Otherwise, observers can be used to estimate the signals.

4.1. Properties of model-free robust decentralised control

4.1.1. Stability. Assuming Lyapunov stability holds in the inner loop, then the outer loop (i.e. whole system) stability is Hurwitz stable. This can be briefly proved, by considering the whole system transfer function matrix $G = C_{IV}[I_n + C_{IV}]^{-1}C_{NDII} = C_{IV}[I_n + C_{IV}]^{-1}\big|_{C_{NDII}=I_n}$. The system is Hurwitz stable, once the C_{IV} is assigned to make $[I_n + C_{IV}]$ a matrix with all eigenvalues satisfy $\text{Re}(\lambda_j) < 0$, $\forall \lambda_j \in [I_n + C_{IV}]$. For example, a second order controller $C_{iIV}(\zeta_i, \omega_{in})$ gives the ith subsystem an ordinary differential equation $\ddot{y} + 2\zeta\omega_n\dot{y} + \omega_n^2 y = 0, \zeta, \omega_n \in \mathbb{R}^+$.

4.1.2. Robustness against internal uncertainty. It has much greater robustness compared with model-based approaches, including online-model approaches. This is because those using nominal model to determine the equivalent control in SMC deal with percentage uncertainty with $\frac{|UC|}{|NM|+|UC|} < 100\%$ ($|UC|$ and $|NM|$ are the absolute values of uncertainty and nominal model, respectively), and the model-free approach deals with $\frac{|NM|+|UC|}{|NM|+|UC|} = 100\%$ uncertainty in its design, accordingly, it can be considered as a full/total robust control approach.

4.1.3. Robustness against external disturbance. The double loops have robustness against disturbances, SMC in the inner loop has its own inherent robustness against disturbances, and the invariant controller in the outer loop can be designed to deal with disturbances. Take a level disturbance d for instance, most encountered in applications, for one of the subsystems, express its closed loop Laplace transfer function as $Y_i(s) = \frac{\omega_n^2 R_i(s)}{s^2+2\zeta\omega_n s+\omega_n^2} + \frac{s(s+2\zeta\omega_n)D(s)}{s^2+2\zeta\omega_n s+\omega_n^2}\Big|_{C_{iIV}=\frac{\omega_n^2}{s(s+2\zeta\omega_n s)}}$. This shows that the disturbance impact to the output $Y_{dis}(s) = \frac{s(s+2\zeta\omega_n)D(s)}{s^2+2\zeta\omega_n s+\omega_n^2}$ is the asymptotically decayed to zero with the time increasement ($y_{dis}(\infty) = \lim_{s\to 0} sY_{dis}(s) = \lim_{s\to 0} \frac{s(s+2\zeta\omega_n)d}{s^2+2\zeta\omega_n s+\omega_n^2} = 0$), which is due to the integral control to suppress the disturbance.

5. Case studies

5.1. Description of the dynamic plants

Two two-input-two-output (TITO) model-unknown (models are only used for simulations, rather than designing the corresponding control systems) nonlinear dynamic plants are selected for the bench test of the designed decentralised control systems.

5.1.1. Coupled inverted pendulum system. As shown in Figure 3, two inverted pendulums connected by a spring, each is controlled by a torque ($u_i, i = 1, 2$) generated from a servomotor at the pivot. This plant has been used as a typical bench test example for decentralised control of interconnected nonlinear systems (Spooner and Passino, 1999; Ding et al. 2021; Li et al., 2021). The state space model is expressed as

$$P_{11}: \begin{cases} \dot{x}_{11} = x_{12} \\ \dot{x}_{12} = \left(\frac{m_1 gr}{J_1} - \frac{kr^2}{4J_1}\right)\sin(x_{11}) + \frac{kr}{2J_1}(l-b) + \frac{u_1}{J_1} \\ \qquad\quad + \frac{kr^2}{4J_1}\sin(x_{21}) \\ y_1 = x_{11} \end{cases}$$

$$P_{12}: \begin{cases} \dot{x}_{21} = x_{22} \\ \dot{x}_{22} = \left(\frac{m_2 gr}{J_2} - \frac{kr^2}{4J_2}\right)\sin(x_{21}) - \frac{kr}{2J_2}(l-b) + \frac{u_2}{J_2} \\ \qquad\quad + \frac{kr^2}{4J_2}\sin(x_{11}) \\ y_2 = x_{21} \end{cases} \quad (5.a)$$

where $y_i = x_{i1} = \theta_i, i = 1,2$ are the angular positions, $\dot{y}_i = x_{2i} = \dot{\theta}_i, i = 1,2$ are the angular rotational speeds, and $u_i, i = 1,2$ are the torques. The simulation initial state matrix is set with $x(0) = \begin{bmatrix} x_{11} = 1 & x_{12} = 0 \\ x_{21} = -0.8 & x_{22} = 0 \end{bmatrix}$ (Ding et al. 2021). Table 1 lists the rest of the parameters.

5.1.2. Coupled non-affine nonlinear dynamic plan. This plant is described below,

$$P_2 : \begin{cases} \ddot{y}_1 + y_2\dot{y}_1 + u_1\dot{y}_2 + 0.6y_1 - \sin(u_1) - 2u_1 - u_1^3 = 0 \\ \ddot{y}_2 - 1.5\left(1 - y_2^2\right)\dot{y}_2 + y_1 - 2u_2 + e^{\left(-u_2^2\right)} - u_2^3 = 0 \end{cases} \tag{5.b}$$

Inspect the input-output model of (5.b), the first line of the system is a non-affine nonlinear dynamic sub-plant, and the second line is an expanded Van der Pol equation with nonlinear control input, the interactions/couplings are the two outputs appearing in both lines of the equations.

5.2. Model-free robust decentralised control system design

The aim of the case study is the conducting of computational experiments, that is, Simulink-platformed demonstrations of the proposed MFRDC and analysis of numerically generated plots in relation to those theoretically derived/proved. There are several objectives to enable the case study to demonstrate the MFRDC of the interconnected nonlinear dynamic systems.

1) The specified system performance is well achieved for tracking control, that is, $Y_1 = \frac{C_{1IV}}{1 + C_{1IV}} R_1$ $Y_2 = \frac{C_{2IV}}{1 + C_{2IV}} R_2$ (dynamic performance in terms of Laplace transform) $\lim_{t \to \infty} \mathrm{diag}[\, e_1(t) \quad e_2(t)\,] = \lim_{t \to \infty} \mathrm{diag}[\, r_1(t) - y_1(t) \quad r_2(t) - y_2(t)\,] \to 0_2$ (steady state performance).
2) Generality of the MFRDC framework in the control system design, including the tests of the functional components of model-free NDII, U-control configuration with NDII, and invariant controller (IC). Further this once-off design is applicable to both cases.
3) Test robustness with unknown plant and external disturbance, and even further switched unknown nonlinear dynamics.

Assume the dynamic order of each subsystem known, the state/output derivatives are measurable, otherwise some types of observers can be taken in to estimate (Fareh et al. 2021).

To achieve the above objectives, set up the simulation platform with

1) For both case studies, setup two references with

$$r_1(t) = \begin{cases} 2, t = [0, \cdots 10] \\ 0, \text{otherwise} \end{cases} \quad r_2(t) = \begin{cases} 1, t = [3, \cdots 10] \\ 0, \text{otherwise} \end{cases}$$

2) Assign the error vector $\tilde{y}_i = [\, e_i \quad \dot{e}_i\,]^T = [\, y_i - y_{id} \quad \dot{y}_i - \dot{y}_{id}\,]^T, i = 1,2,$ where y_i and y_{id} are the measured output and the desired output, respectively. Select the corresponding sliding functions as $\sigma_i(\tilde{y}_i) = 10e_i + \dot{e}_i, i = 1,2$ and the sliding-mode boundary layer thickness $\delta_1 = \delta_2 = 1$.

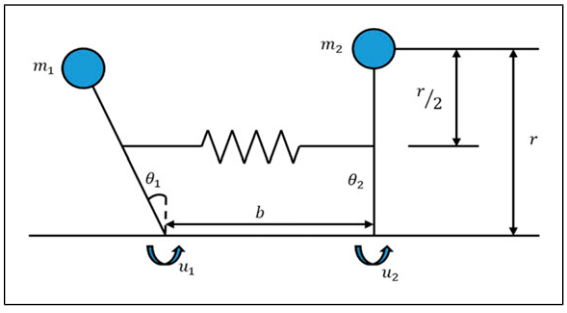

Figure 3. Coupled inverted pendulums.

Table 1. Parameters of the inverted pendulums.

Parameters	Names
$m_1 = 2$ kg, $m_2 = 2.5$ kg	End mass of pendulum
$J_1 = 0.5$ kg · m^2, $J_2 = 0.625$ kg · m^2	Moment of inertia
$g = 9.81$ m/s^2	Gravitational acceleration
$k = 100$ N/m, $l = 0.5$ m	Connecting spring constant, natural length
$r = 0.5$ m	Pendulum height
$b = 0.5$ m	Distance between the pendulum hinges

3) Design of the NDII, assign the SMC gains, by a few of trial-and-error tunings, for both systems $k_{1g} = -15 \quad k_{1p} = -15 \quad k_{1i} = -10$ $k_{2g} = -15 \quad k_{2p} = -15 \quad k_{2i} = -10$. It should be noted that the trial-and error tuning has lager range of selections because of the design is based the Lyapunov differential inequality $\dot{V} = \dot{\sigma}\sigma < 0$, the system output performance is not changed since the specification of the IC in the outer loop. Consequently, the parameter set tuning is robust and flexibly easy.
4) Design of the invariant controller, assign two second order IC as $C_{iIV} = \frac{\omega_{in}^2}{s(s+2\zeta_i\omega_{in})}, i = 1, 2,$ where the damping ratios ζ_i and the undamped natural frequencies ω_{in} are specified with $\zeta_1 = 1.03 \quad \omega_{1n}^2 = 7$ $\zeta_2 = 1.10 \quad \omega_{2n}^2 = 8$ for the first system (two monotonic responses), and $\zeta_1 = 0.7 \quad \omega_{1n}^2 = 1\zeta_2 = 1\omega_{2n}^2 = 1$ for the second system (the first output with decayed oscillatory response and the second output with monotonic response, respectively). The designed ICs are also used to provide the desired state vectors for the NDIIs in the inner loops, that is, $x_{id} = [x_{id1} \quad x_{id2}]^T = \left[\frac{1}{s} \quad \frac{\omega_{in}^2}{s+2\zeta_i\omega_{in}}\right]^T, i = 1, 2.$

5.3. Analysis of simulation demonstrations

5.3.1. Analysis and comparison of control system 1. Figure 4 shows the simulated results with the proposed MFRDC/U-control and Figure 5 shows the plots generate by a well-known mode-based SMC (Ding et al. 2021). A summary report is presented below.

1) The insight of the MFRDC composed of the NDII and the U-control work effectively to achieve the control system objectives 1, 2, and 3.
2) The transient response and the steady state errors are accommodated well with the specified control system performance without involving the plant model (treated as whole uncertainty) in design.
3) The NDII clearly shows the conciseness and robustness of the nonlinear dynamic inversion and decoupling, which is the kernel foundation for achieving the system tracking specifications. This gives a far-reaching view that without a model, dynamic inversion is still achievable and robustly computational effective, it is noted that the model-free dynamic inversion needs to be implemented in closed loop configuration. There is no chattering effect and large control inputs observed.

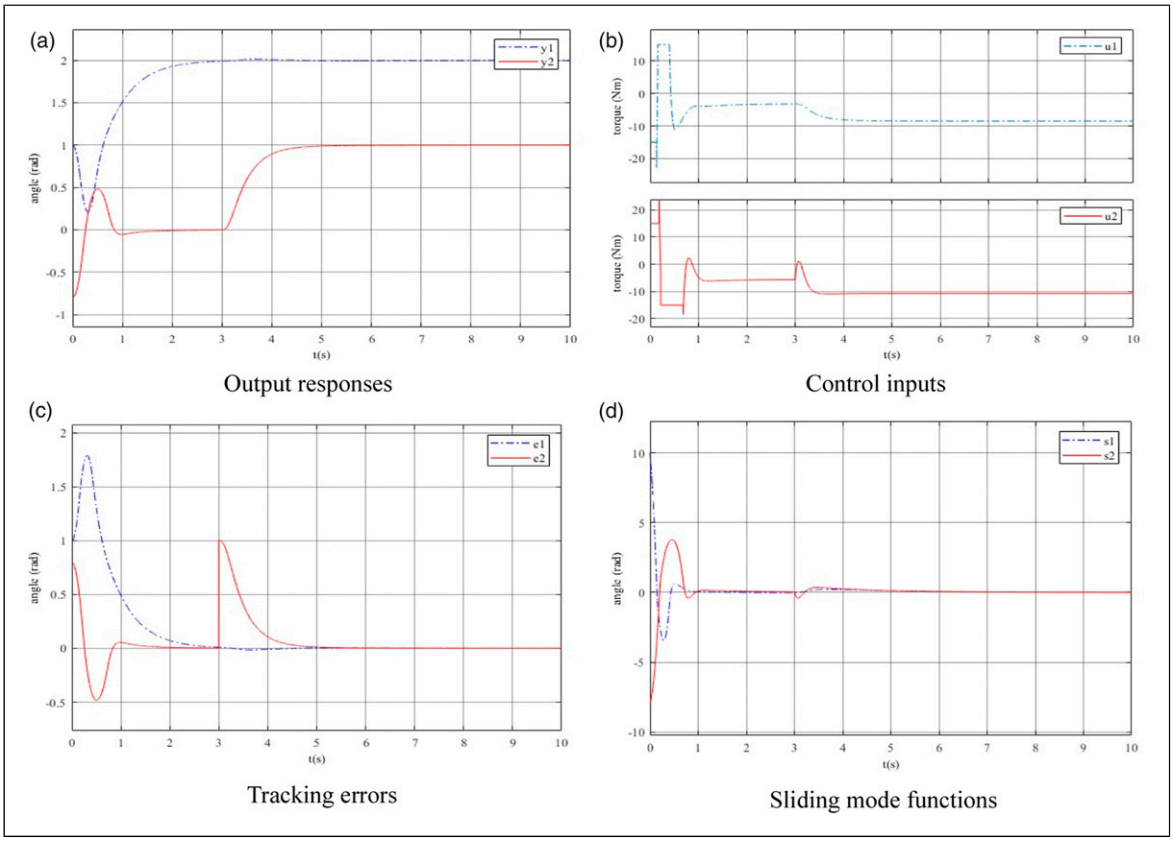

Figure 4. Case1 – MFRDC of coupled inverted pendulums. (a) Output responses, (b) control inputs, (c) tracking errors, and (d) sliding mode functions.

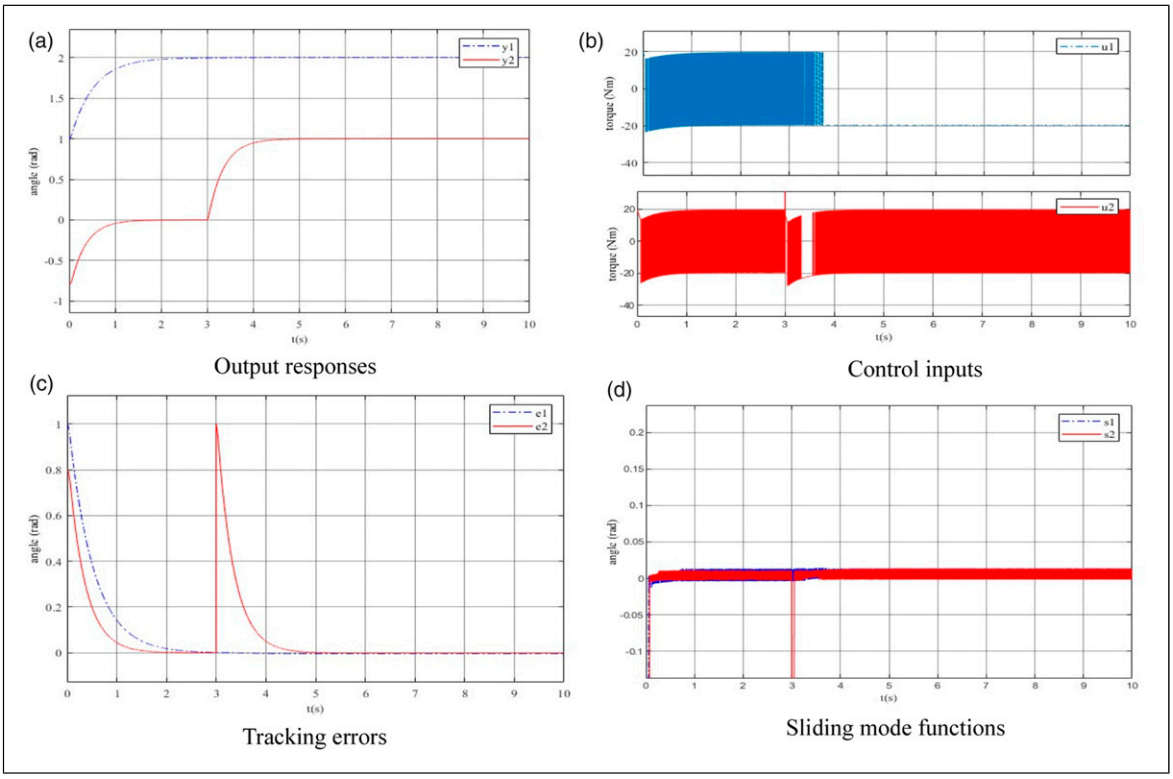

Figure 5. Case1 – Model-based SMC of coupled inverted pendulums (Ding et al. 2021). (a) Output responses, (b) control inputs. (c) tracking errors, and (d) sliding mode functions.

4) Compare the U-control with the recently published representative model-based SMC (Ding et al. 2021) on the same inverted pendulum, which the simulation plots are shown in Figure 5. To obtain the similar results, the conventional model-based SMC design requires (1) the nominal isolated subsystem models to single out uncertainty models, (2) matched uncertainty known, (3) all uncertainty bounds known, (4) large control output oscillation to achieve the specified system outputs, (5) the model-based SMC design need more design parameters for running the simulation platform, and (6) if system changed, the above requests must be updated accordingly. There are two comparative merits with the model-based SMC, (1) it performs better in accommodating initial states from comparing plots (a) in Figures 4 and 5, and (2) the terminal SMC provides a good reference for expanding the U-control into finite time SMC in the following studies.
5) For adaptive fixed-time neural network control (AFTNNC) (Li et al., 2021), the design requires (1) neural network assignment (nodes, layers, etc.) and data-based iteration to estimate uncertainties, (2) fixed-time lowpass filter, (3) an adaptive backstepping routine to cope with unknown system in fixed-time settings, and (4) again the model-based approach need repeat the above procedures once a system model changed. Obviously, the new design approach need uncertainty known or estimated in advance in control execution, plus the complex routines in the control system configurations model by model. One more negative point on the AFTNNC is that it is not practical for this case application as its control input require large torques. It should be noted that due to the length of the paper, the AFTNNC configuration is shown in Figure 8 and the simulation plots are shown in Figure 9 in appendix.
6) In summary, the compared approaches require extra effort and expertise (e.g. requiring the uncertainty bound known or to be estimated), which are unnecessary with the U-control, to deal with uncertainties in the control system designs. It should be noted that the compared two approaches do not need decoupling the dynamic plant, which could be significant challenge to model-based control system design. However, U-control does not suffer such technical complexity as this is naturally embedded in the model-free NDII.

5.3.2. Analysis of control system 2. Figures 6 and 7 show the simulated results. Because this is a numerical example, there are no physical units in the horizontal and vertical coordinates. A summary report is presented below.

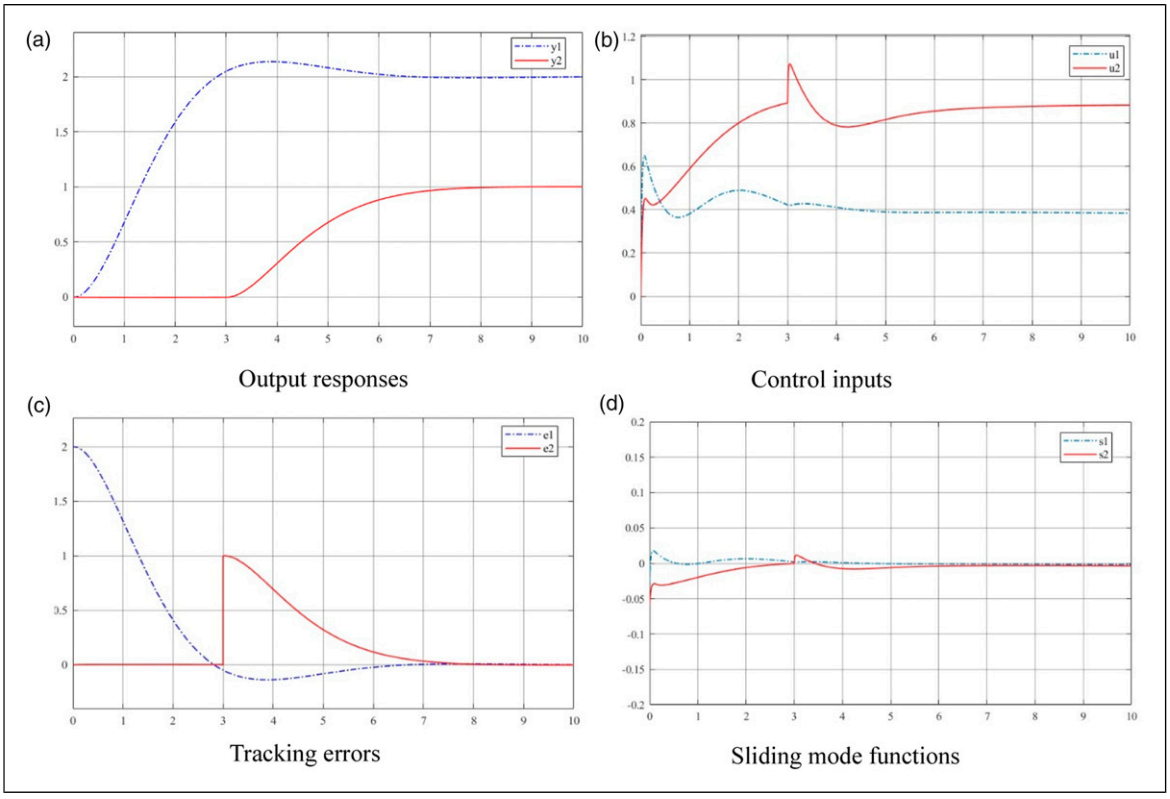

Figure 6. Case2 – MFRDC of coupled non-affine nonlinear dynamics. (a) Output responses, (b) control inputs, (c) tracking errors, and (d) sliding mode functions.

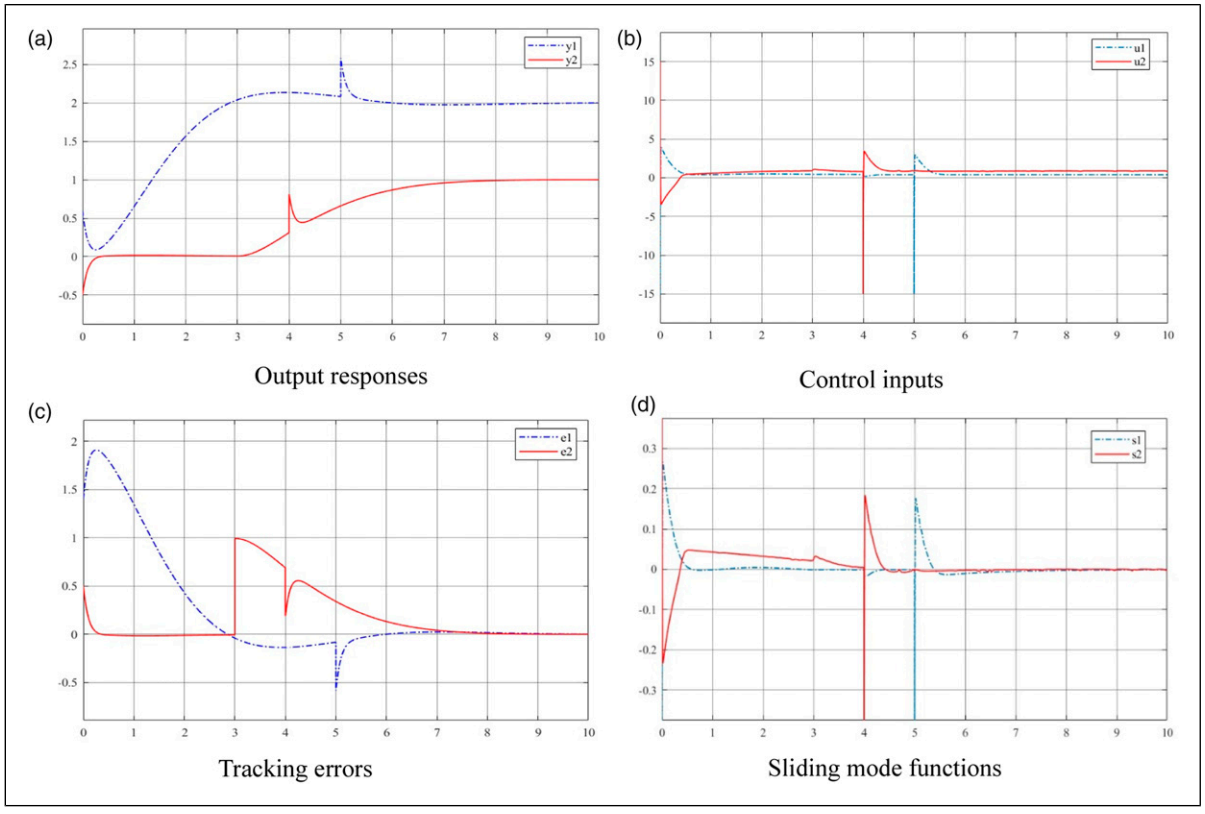

Figure 7. Case2 – MFRDC of coupled non-affine nonlinear dynamics with non-zero initial states and disturbances. (a) Output responses, (b) control inputs, (c) tracking errors, and (d) sliding mode functions.

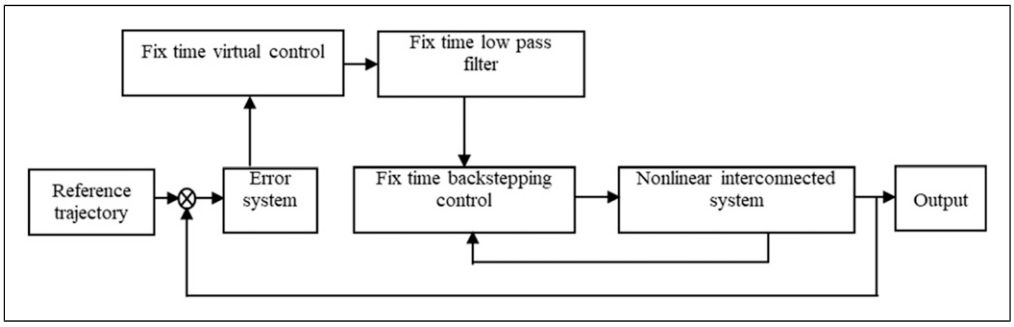

Figure 8. The adaptive control system.

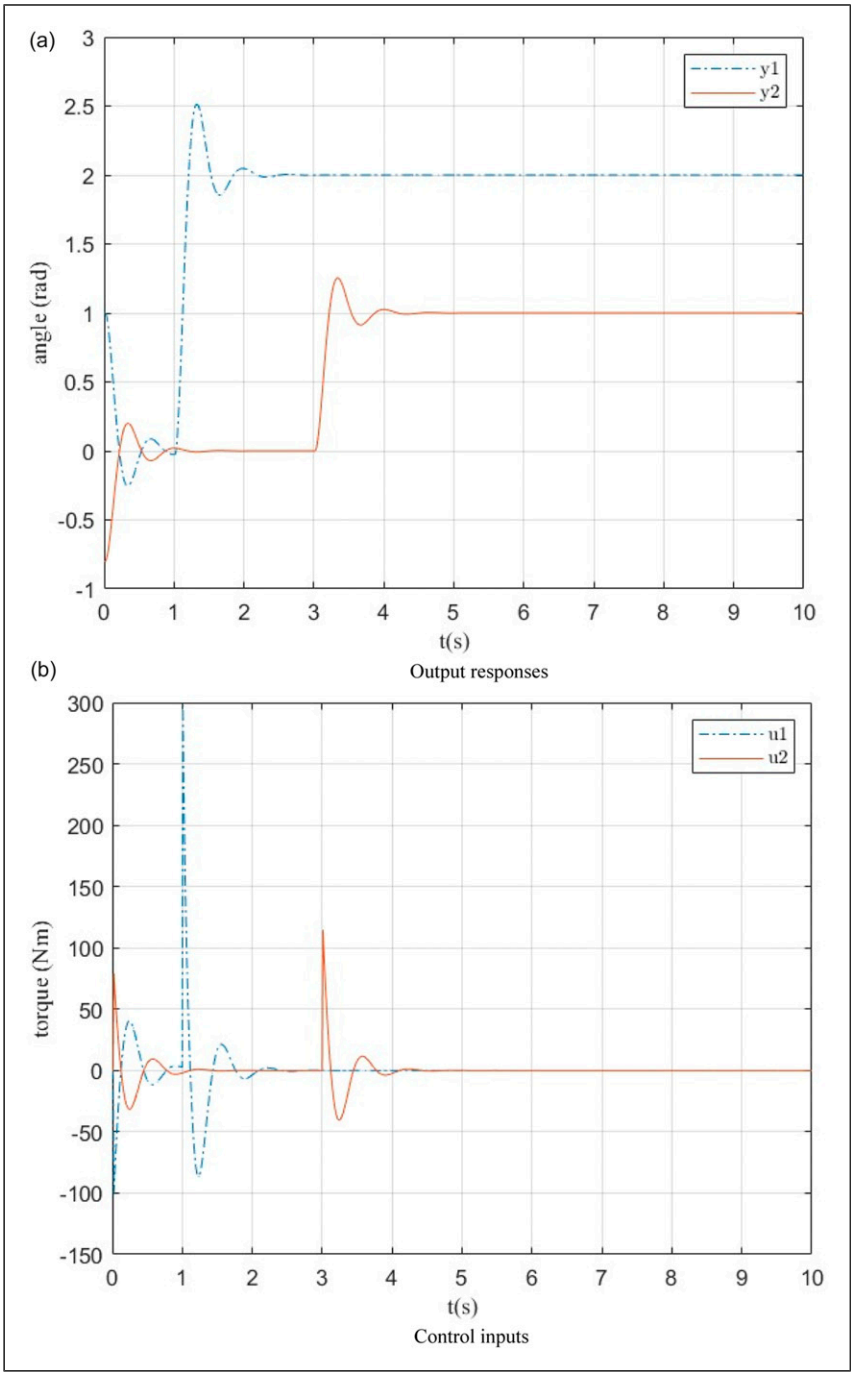

Figure 9. Case1 – Adaptive control of coupled inverted pendulums (Li et al., 2021). (a) Output responses and (b) control inputs.

1) The specified performances, as shown in system one, are demonstrated, which has no need to be repeated. The MFRDC is applicable to non-affine nonlinear dynamic plants without extra effort in configuration and design, which the output response performance is effectively specified by assigning the damping ratio and the undamped natural frequency, without involving any plant.
2) Figure 9 shows the tests on the second example with (1) non-zero initial states $(y_1(0) = 0.6, y_2(0) = -0.5)$, which is very possible for some plants with non-zero initial states, and (2) simultaneously, the external constant disturbances $d_1(t) = 0.5, t \geq 5, d_2(t) = 0.5, t \geq 4$ added, which is a popular form of disturbance in practice, and are suppressed to zero because the integral function in the invariant controllers. Inspection of the plots in Figure 9, the MFSMC is still working well with the expected outcomes.
3) The who simulation clearly demonstrates the merits of the model-free method in general control system design (because of no request on the system/model structures and parameters) and stronger robustness against model uncertainties (because of the underlaying plants treated as whole uncertainty), which the two examples can be considered as one system with two separate dynamics, that is, Case 1 takes on in time duration of 0–10 and the Case 2 is switched on from 10 and kept till time instance 20.
4) For both cases, the outer loop of the invariant controller favourably plays the roles 1) specifying the whole control system output dynamic/static performance, suppressing the external constant disturbance, and 3) providing the desired state vector for nonlinear dynamic, interaction inversion (NDII) in the inner loop.

6. Conclusions

The presented method could be expanded to provide solutions for the other related issues in MIMO control system design, such as under-actuated control, over-actuated control, and particularly decoupling control for plants with additional input-output coupling, beyond just the output dynamic coupling encountered in this study. In addition, (1) the model-free control methodology has roots in bionics, which effectively uses the error and the error derivatives, in conjunction with SMC and PID heuristic behaviour. This merit is comparable to mode-free adaptive control, which would still need online model updating with measured errors and the model variables, and the other data-driven learning control approaches requiring online model estimation, (2) the U-control configuration represents a fundamental insight – the control system design is a backward procedure to invert a system with prespecified requests, U-control takes an inverting procedure in $[AB]^{-1} \rightarrow^{U-control} [A]^{-1}[B]^{-1}$, which could provide a co-design platform for effective, rapid, independent design of plant and control and (3) The approach does not conflict with model-based methods: in general, it seamlessly supplements the methods across the whole spectrum from model-based to mode-free. Hopefully, these insights could provide supplementary references for other control approaches in strategic methodology development.

Acknowledgements

The authors would like to express their gratitude to the editors and the anonymous reviewers for their helpful comments and constructive suggestions regarding the revision of the paper. The second author is grateful to the partial PhD studentship from the Engineering Modelling and Simulation Research Group of the University of the West of England, UK. The authors greatly appreciate Dr Steve Wright for proof-reading the revised draft.

Declaration of conflicting interests

The author(s) declared no potential conflicts of interest with respect to the research, authorship, and/or publication of this article.

Funding

The author(s) received no financial support for the research, authorship, and/or publication of this article.

ORCID iDs

Quanmin Zhu https://orcid.org/0000-0001-8173-1179
Ruobing Li https://orcid.org/0000-0002-5154-007X
Jianhua Zhang https://orcid.org/0000-0002-6561-5917
Baiyang Shi https://orcid.org/0000-0003-0577-2977

References

Antonelli G (2013) Interconnected dynamic systems: an overview on distributed control. *IEEE Control Systems Magazine* 33(1): 76–88. DOI: 10.1109/MCS.2012.2225929.

Bakule L (2008) Decentralized control: an overview. *Annual Reviews in Control* 32(1): 87–98. DOI: 10.1016/j.arcontrol.2008.03.004.

Bakule L (2014) Decentralized control: status and outlook. *Annual Reviews in Control* 38(1): 71–80. DOI: 10.1016/j.arcontrol.2014.03.007.

Chen B, Hu G, Ho DW, et al. (2021) Distributed estimation and control for discrete time-varying interconnected systems. *IEEE Transactions on Automatic Control* 67(5): 2192–2207. DOI: 10.1109/TAC.2021.3075198.

Ding Y, Yan X, Mao Z, et al. (2021) Decentralised sliding mode tracking control for a class of nonlinear interconnected systems. *2021 American Control Conference (ACC)*. New Orleans, LA: IEEE, pp. 2157–2162. DOI: 10.23919/ACC50511.2021.9483425.

Dong B, An T, Zhou F, et al. (2019) Model-free optimal decentralized sliding mode control for modular and reconfigurable robots based on adaptive dynamic programming. *Advances in*

Mechanical Engineering 11(12): 1687814019896923. DOI: 10.1177/1687814019896923.

Fareh R, Khadraoui S, Abdallah MY, et al. (2021) Active disturbance rejection control for robotic systems: a review. *Mechatronics* 80: 102671. DOI: 10.1016/j.mechatronics.2021.102671.

Guo BZ and Zhao ZL (2011) On the convergence of an extended state observer for nonlinear systems with uncertainty. *Systems & Control Letters* 60: 420–430.

Hua CC, Li QD and Li K (2021) Event-based finite-time control for high-order interconnected nonlinear systems with asymmetric output constraints. *IEEE Transactions on Automatic Control* 67(11): 6135–6142. DOI: 10.1109/TAC.2021.3128471.

Hussain NAA, Ali SSA, Ovinis M, et al. (2019) Underactuated coupled nonlinear adaptive control synthesis using U-model for multivariable unmanned marine robotics. *IEEE Access* 8: 1851–1865. DOI: 10.1109/ACCESS.2019.2961700.

Jokić A and Nakić I (2019) On structured Lyapunov functions and dissipativity in interconnected LTI systems. *IEEE Transactions on Automatic Control* 65(3): 970–985. DOI: 10.1109/TAC.2019.2915751.

Li R, Zhu QM, Kiely J, et al. (2020) Algorithms for U-model-based dynamic inversion (UM-dynamic inversion) for continuous time control systems. *Complexity*: 1–14. DOI: 10.1155/2020/3640210.

Li Y, Zhang J, Xu X, et al. (2021) Adaptive fixed-time neural network tracking control of nonlinear interconnected systems. *Entropy* 23(9): 1152. DOI: 10.3390/e23091152.

Li R, Zhu QM, Zhang W, et al. (2022) An improved U-control design for nonlinear systems represented by input/output differential models with a disturbance observer. *International Journal of Control*: 1–12. DOI: 10.1080/00207179.2022.2111370.

Li R, Zhu QM, Hamidreza N, et al. (2023) Trajectory tracking of a quadrotor using extend state observer based U-model enhanced double sliding mode control. *Journal of the Franklin Institute* 360(4): 3520–3544.

Ma HJ and Xu LX (2020) Decentralized adaptive fault-tolerant control for a class of strong interconnected nonlinear systems via graph theory. *IEEE Transactions on Automatic Control* 66(7): 3227–3234. DOI: 10.1109/TAC.2020.3014292.

Mukherjee S, Bai H and Chakrabortty A (2020). Model-free decentralized reinforcement learning control of distributed energy resources. In 2020 IEEE Power & Energy Society General Meeting (PESGM), Montreal, Canada, 2-6 Aug. 2020. 1-5. DOI: 10.1109/PESGM41954.2020.9281968.

Slotine JJE and Li W P (1991) *Applied Nonlinear Control*. Prentice Hall.

Spooner JT and Passino KM (1999) Decentralized adaptive control of nonlinear systems using radial basis neural networks. *IEEE Transactions on Automatic Control* 44(11): 2050–2057. DOI: 10.1109/9.802914.

Wei W, Duan B, Zuo M, et al. (2022) An extended state observer based U-model control of the COVID-19. *ISA Transactions* 124: 115–123. DOI: 10.1016/j.isatra.2021.02.039.

Zhang XM, Han QL, Ge X, et al. (2019) Networked control systems: a survey of trends and techniques. *IEEE/CAA Journal of Automatica Sinica* 7(1): 1–17. DOI: 10.1109/JAS.2019.1911651.

Zhang W, Zhu Q, Mobayen S, et al. (2020). U-Model and U-control methodology for nonlinear dynamic systems. *Complexity*, 2020, 1–13. DOI: 10.1155/2020/1050254

Zhao D and Polycarpou MM (2021) Distributed fault accommodation of multiple sensor faults for a class of nonlinear interconnected systems. *IEEE Transactions on Automatic Control* 67(4): 2092–2099. DOI: 10.1109/TAC.2021.3073284.

Zhu QM (2021) Complete model-free sliding mode control (CMFSMC). *Scientific Reports* 11(1): 22565. DOI: 10.1038/s41598-021-01871-6.

Zhu QM and Guo LZ (2002) A pole placement controller for non-linear dynamic plants. *Proceedings of the Institution of Mechanical Engineers - Part I: Journal of Systems & Control Engineering* 216(6): 467–476. DOI: 10.1177/095965180221600603.

Zhu QM, Mobayen S, Nemati H, et al. (2023) A new configuration of composite nonlinear feedback control for nonlinear systems with input saturation. *Journal of Vibration and Control* 29(5-6): 1417–1430. DOI: 10.1177/10775463211064010.

Appendix

Simulation for Case 1 by adaptive fixed-time neural network tracking control of nonlinear interconnected systems (Li et al., 2021).